Supplementary Information

Synthesis of $(Ga_{1-x}Zn_x)(N_{1-x}O_x)$ with Enhanced Visible-Light Absorption and Reduced Defects by Suppressing Zn Volatilization

Dennis P. Chen and Sara E. Skrabalak*

Table of Contents

FTIR spectrum of ZnGa-LDH (Figure S1)	S2
Assignment of the main IR vibration modes of ZnGa-LDH (Table S1)	S2
Pawley refinement of ZnGa-LDH high resolution synchrotron XRD data (Figure S2)	S3
STEM micrographs/EDS-mapping of GZNO-NH_3 and GZNO-O_2 /NH_3 (Figure S3)	S4
Reaction time studies of GZNO-NH_3 and GZNO-O_2/NH_3 monitored ex situ by XRD (Figure S4).	S5
Powder patterns of GZNO-O_2/NH_3 particles obtained from various nitridation times (Figure S5)	S6
XPS spectra of GZNO particles (Figure S6)	S7-8
Zn fraction in GZNO samples as determined by ICP-OES and XPS elemental analysis (Table S2)	S8
XRD patterns of GZNO obtained from the nitridation of ZnGa-LDH (Figure S7)	S9
Reliability values for Pawley refinements fitted to synchrotron GZNO-NH_3 data comparing the relevance of each anisotropic broadening parameter (Table S4)	S10
References	S10

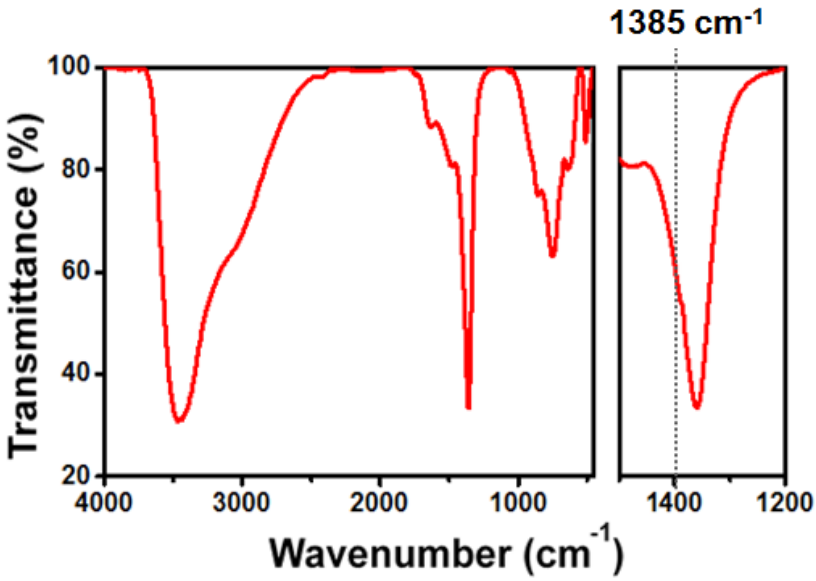

Figure S1. FTIR spectrum of ZnGa-LDH plates. The right panel is a zoom-in view highlighting the carbonate anion stretching mode and the absence of an N-O stretch (1385 cm^{-1}).

Table S1. Assignment of the main IR vibration modes of ZnGa-LDH.

Vibration Modes	Resonance Frequency (cm^{-1})
υ[O-H]	3446
υ[H-O-H]	1637
υ[N-O]	(1385)
$\upsilon[C\text{-}O]_s$	1358
υ[M-O]	735

The ZnGa-LDH sample displays a strong absorption with a broad profile in the 3490-3440 cm^{-1} region, associated with the presence of H-bonding interactions between the interlamellar water molecules and the OH functional groups of the hydroxide-based layers.[1] Absorption at the lower wavenumbers between 740-485 cm^{-1} is attributed to the vibrational modes associated with the $M(OH)_6$ complexes.[2] More specifically, the carbonate species intercalated between the hydroxide layers show a strong intensity band at ca. 1358 cm^{-1}, which is typical for the carbonate's υ_3 stretching mode.[3] As can be seen in the zoom-in view of the spectra, no band at 1385 cm^{-1}, corresponding to the nitrate's υ_3 stretching mode can be observed.[4]

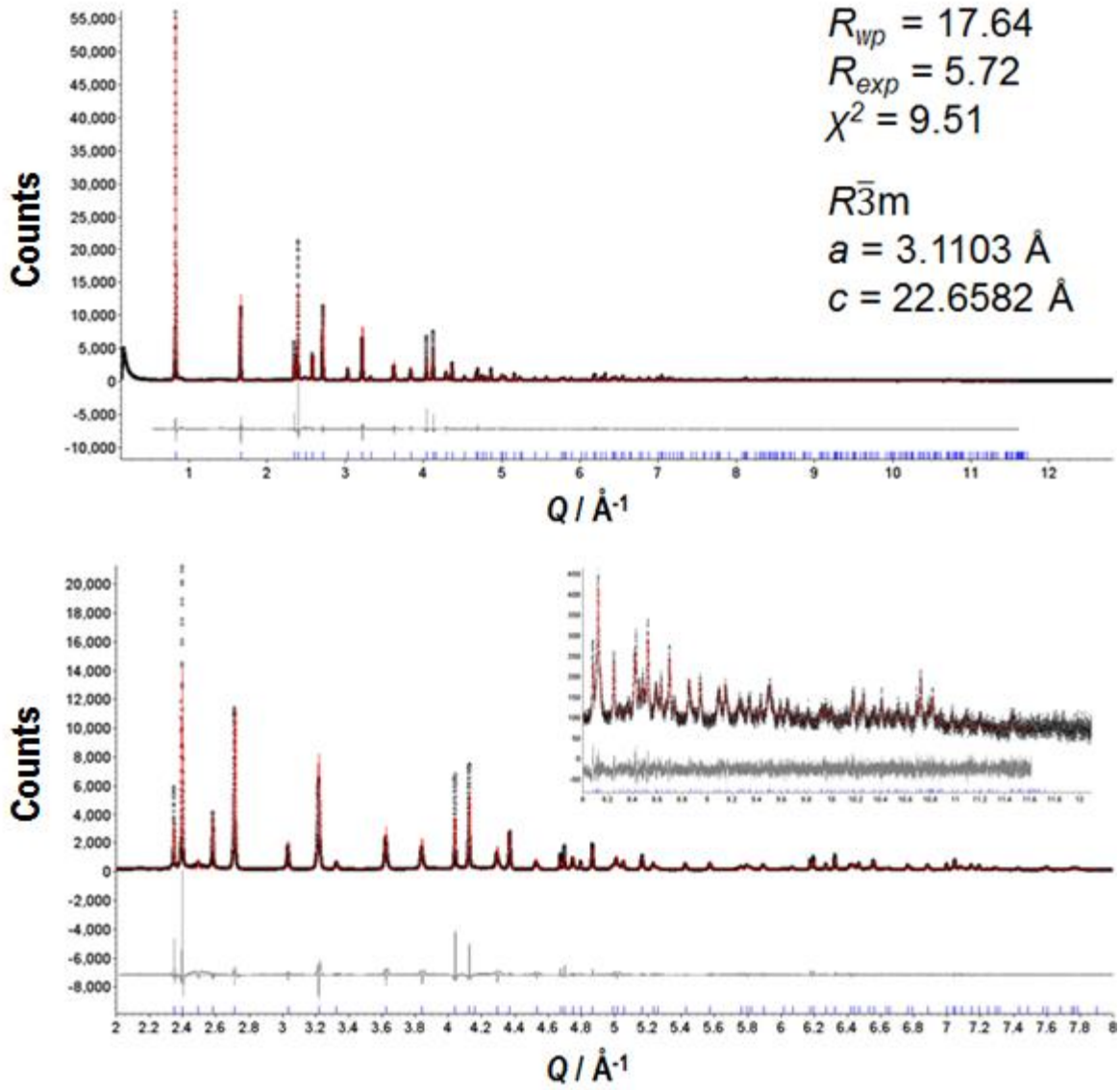

Figure S2. Pawley refinement of ZnGa-LDH high resolution synchrotron XRD data. Whole powder pattern (a), *Q*-range 2-8 Å^{-1} (b), and *Q*-range 8-12.1 Å^{-1} (b, inset), respectively. Markers represent experimental data, while the solid red lines indicate the calculated pattern. The difference pattern is shown in gray below the experimental and calculated patterns. The high-*Q* region of the powder pattern is shown in the inset.

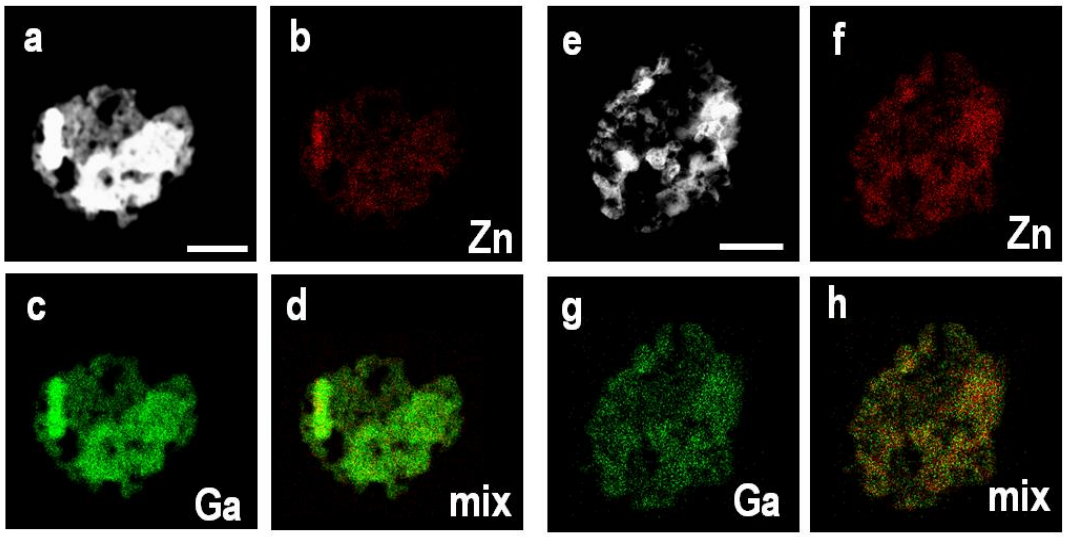

Figure S3. STEM micrographs/EDS-mapping of GZNO-NH_3 (a-d) and GZNO-O_2 /NH_3 (e-h). Scale bars = 200 nm.

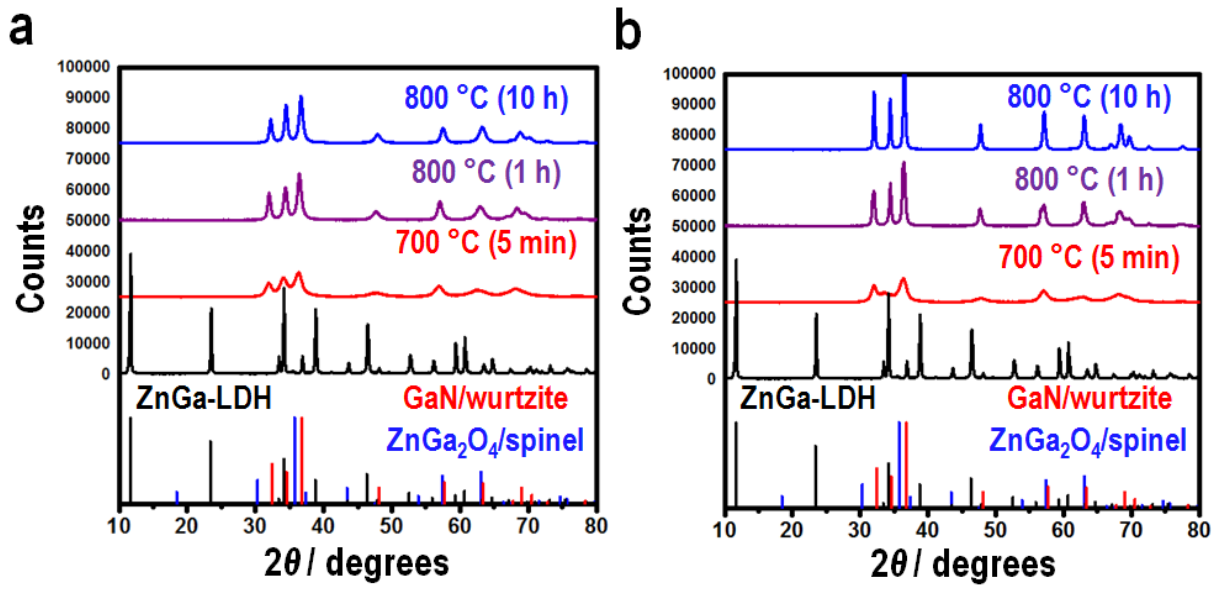

Figure S4. Reaction time studies monitored ex situ by XRD. Powder patterns of the set of reactions for GZNO-NH_3 (a) and GZNO-O_2/NH_3 (b). The data sets are identical to those shown in Figure 2, but left uncropped to show the entire range of 10-80 °2θ. The black patterns corresponds to the precursor ZnGa-LDH while the red and blue pattern belongs to particles that were quenched at 700 °C (red) and 800 °C after 1 h (purple), respectively. The blue pattern corresponds to GZNO and GZNO-O_2 particles that were nitridated for 10 h. Reference patterns were obtained from ICDD PDF No. 01-076-3644, ICDD PDF No. 01-071-0843, and ICDD PDF No. 01-070-2546 which corresponds to rhombohedral-phase ZnGa-LDH phase (black), spinel $ZnGa_2O_4$ phase (blue), and hexagonal wurtzite GaN (red), respectively.

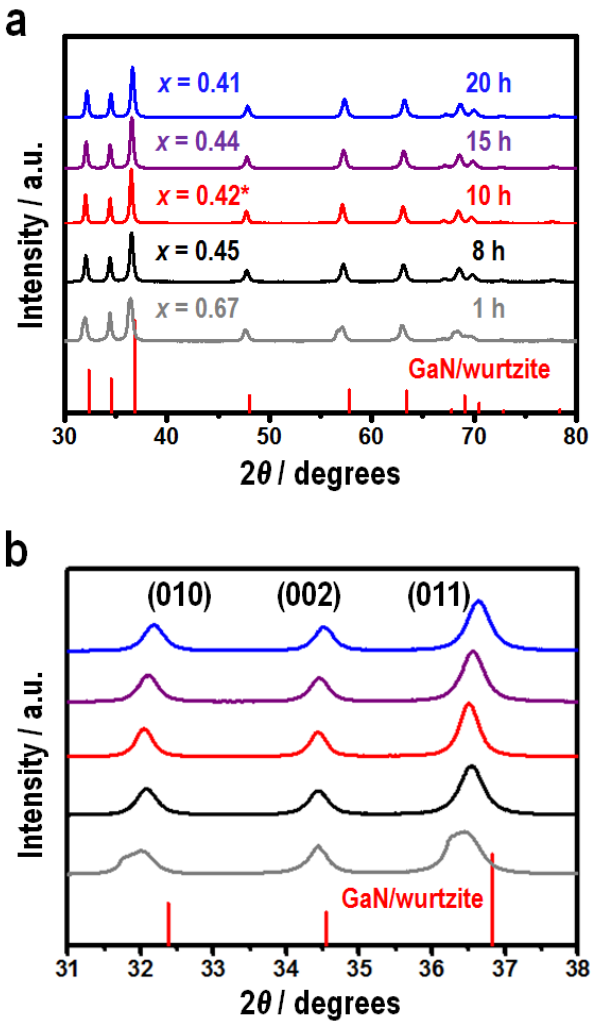

Figure S5. Powder patterns of GZNO-O_2/NH_3 particles obtained from various nitridation times. Powder patterns consisting of the predominant *hkl* reflections are shown in (a), while a narrow 30-40 ° 2θ range is shown in panel (b). The hexagonal wurtzite GaN (red) reference pattern was obtained from ICDD PDF No. 01-070-2546. Zn fractions (x) obtained from SEM-EDS analysis and reaction times are displayed above the corresponding pattern. *Fraction calculated from data obtained from ICP-OES analysis.

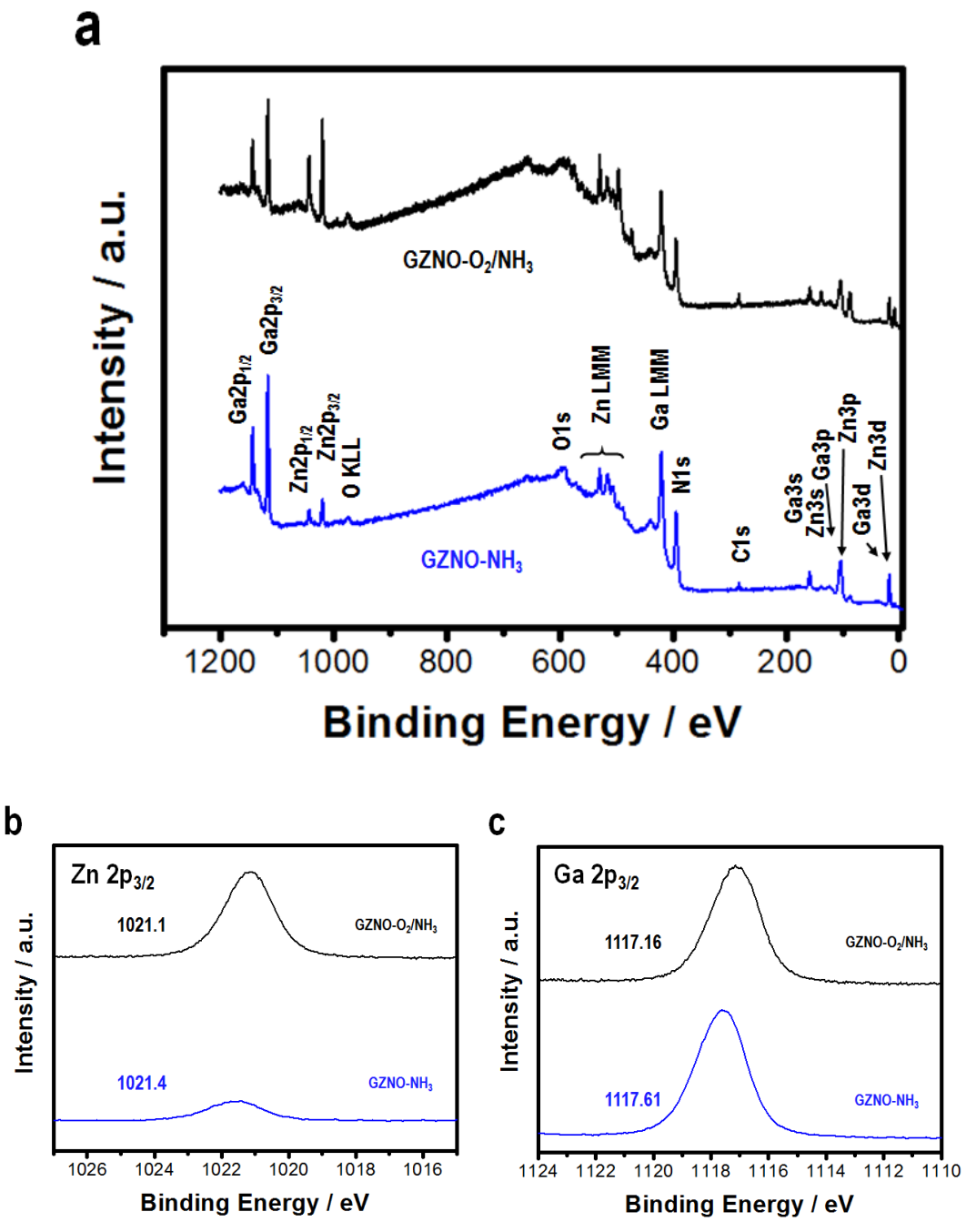
a
Intensity / a.u.
GZNO-O2/NH3
GZNO-NH3
Ga2p1/2
Ga2p3/2
Zn2p1/2
Zn2p3/2
O KLL
O1s
Zn LMM
Ga LMM
N1s
C1s
Ga3s
Zn3s
Ga3p
Zn3p
Ga3d
Zn3d
1200
1000
800
600
400
200
0
Binding Energy / eV
b
Zn 2p3/2
1021.1
GZNO-O2/NH3
1021.4
GZNO-NH3
Intensity / a.u.
1026
1024
1022
1020
1018
1016
Binding Energy / eV
c
Ga 2p3/2
1117.16
GZNO-O2/NH3
1117.61
GZNO-NH3
Intensity / a.u.
1124
1122
1120
1118
1116
1114
1112
1110
Binding Energy / eV

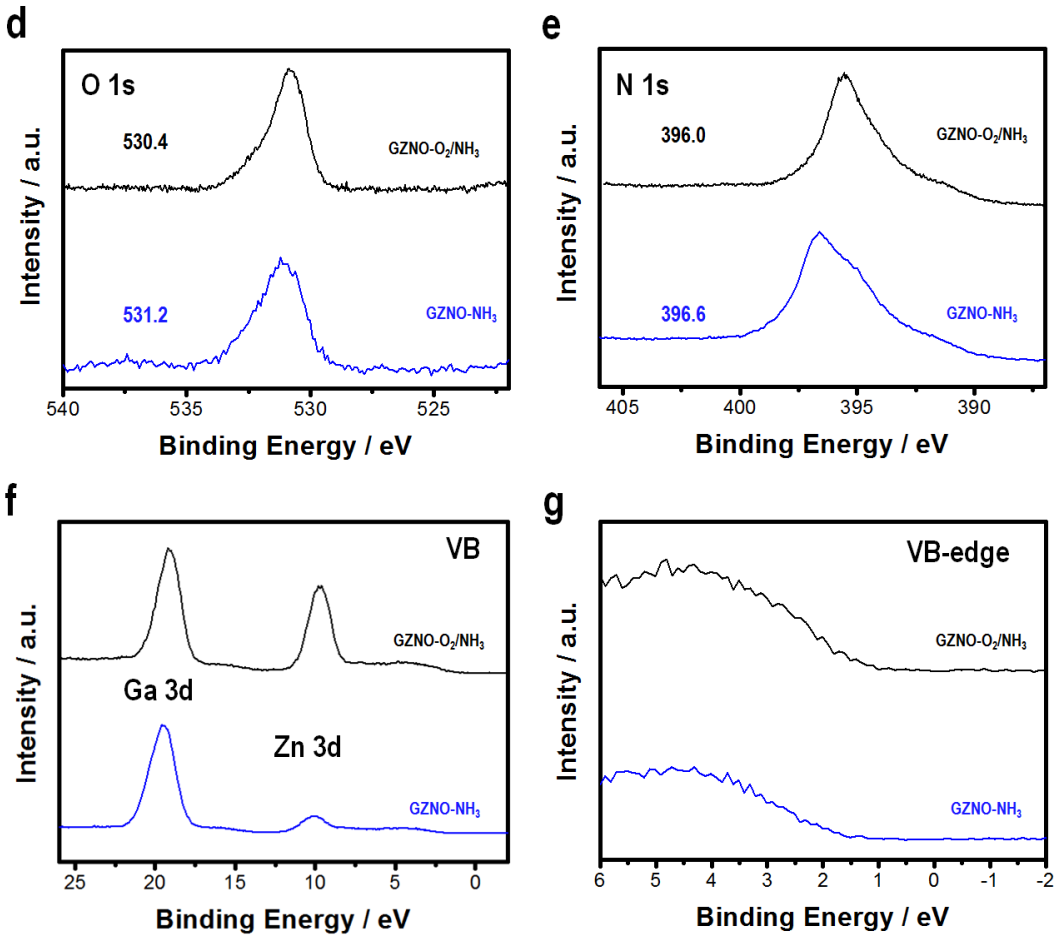

Figure S6. XPS spectra of GZNO particles. Survey scan (a) of GZNO-NH_3 (blue), GZNO-O_2/NH_3 (black), and GZNO-O_2/NH_3/ZnO (red). High resolution scans of the Zn2p (b), Ga2p (c), O1s (d), and N1s (e) lines were obtained. The valence band (VB) region and the VB-edge are shown in panels (f) and (g), respectively.

Table S2. Zn fraction in GZNO samples as determined by ICP-OES and XPS elemental analysis.

Sample ID	Starting Material	ICP-OES Zn/(Zn+Ga)	XPS Zn/(Zn+Ga)
GZNO-NH_3	ZnGa-LDH	0.23	0.14
GZNO-O_2/NH_3	ZnGa-LDH	0.42	0.42

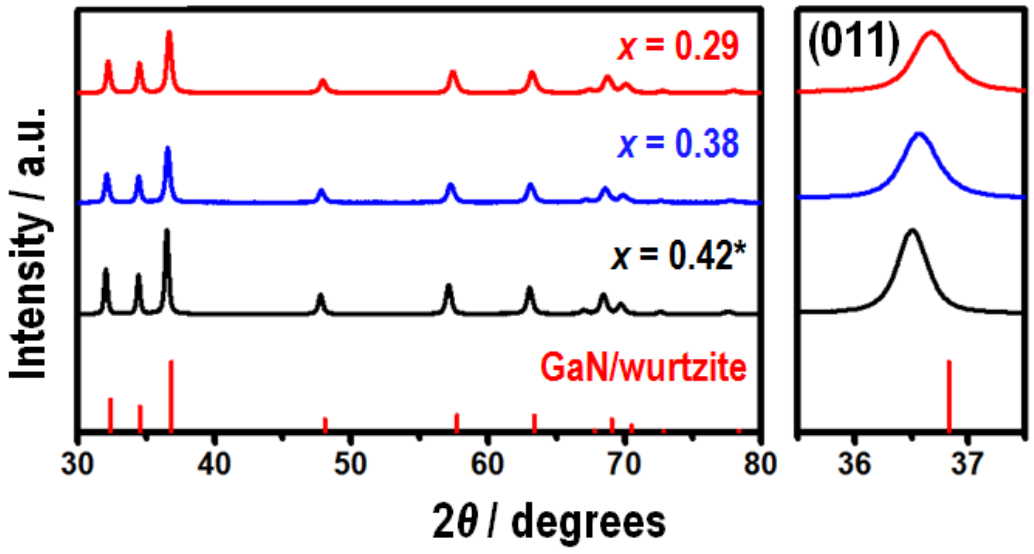

Figure S7. XRD patterns of GZNO obtained from the nitridation of ZnGa-LDH. The black and red patterns represents GZNO-O_2/NH_3 and GZNO-O_2/NH_3 calcined at 800 °C under NH_3 for 5 h. The blue pattern correspond to ZnGa-LDH reacted sequentially with O2/NH3 for 10 h and NH3 for 5 h. Zn fractions (*x*) obtained from SEM-EDS or ICP-OES (*) analysis.

Table S1. Reliability values for Pawley refinements fitted to synchrotron GZNO-NH_3 data with each anisotropic broadening parameters[5] in turn was fixed at zero while the others were refined.

Anisotropic Broadening Parameter	R_{wp}	R_{exp}	χ^2
S_{400}	11.295	7.044	2.571188
S_{202}	11.953	7.044	2.879487
S_{004}	9.599	7.044	1.857006
η	9.474	7.044	1.808956
all used	7.93	7.044	1.267876

Refined Anisotropic Broadening Parameters			
S_{400}	S_{202}	S_{004}	η
16.4×10^4	16.4×10^4	7.8×10^4	0.49

References

1. Ulibarri, M. A.; Hernandez, M. J.; Cornejo, J., Hydrotalcite-like compounds obtained by anion exchange reactions. *J. Mater. Sci.* **1991**, *26*, 1512-1516.

2. Busca, G.; Trifiro, F.; Vaccari, A., Characterization and Catalytic Activity of Cobalt-Chromium Mixed Oxides. *Langmuir* **1990**, *6*, 1440-1447.

3. Hernandez-Moreno, M. J.; Ulibarri, M. A.; Rendon, J. L.; Serna, C., IR characteristics of hydrotalcite-like compounds. *J. Phys. Chem. Miner.* **1985**, *12*, 34-38.

4. Kruissink, E. C. ; Vanreijen, L. L.; Ross, J. R. H., Coprecipitated nickel-alumina catalysts for methanation at high temperature. Part 1.-Chemical composition and structure of the precipitates. *J. Chem. Soc., Faraday Trans.* **1981**, *77*, 649-663.

5. Stephens, P. W., Phenomenological model of anisotropic peak broadening in powder diffraction. *J. Appl. Cryst.* **1999,** *32* (2), 281-289.